



## EPN2020-RI

**EUROPLANET2020 Research Infrastructure**

H2020-INFRAIA-2014-2015

Grant agreement no: 654208

### Deliverable D6.19

#### LMSU contribution to 4th VESPA VA Review Board Report

Due date of deliverable: 31/05/2019

Actual submission date: 05/06/2019

Start date of project: 01 September 2015

Duration: 48 months

Responsible WP Leader: Observatoire de Paris, Stéphane Erard

Project funded by the <i>European Union's Horizon 2020 research and innovation programme</i>		
<b>Dissemination level</b>		
<b>PU</b>	Public	x

<b>Project Number</b>	654208
<b>Project Title</b>	EPN2020 – RI
<b>Project Duration</b>	48 months: 01 September 2015 – 31 August 2019

<b>Deliverable Number</b>	D6.19
<b>Contractual Delivery date</b>	31.05.2019
<b>Actual delivery date</b>	05.06.2019
<b>Title of Deliverable</b>	LMSU contribution to 4th VESPA VA Review Board Report
<b>Contributing Work package(s)</b>	WP6
<b>Dissemination level</b>	Public
<b>Author (s)</b>	Igor Alekseev, Vladimir Kalegaev, Sergey Bobrovnikov, Elena Belenkaya, Aleksander Lavrukhin, David Parunakian, Ivan Pensionerov

**Abstract:**

A wide variety of interactions takes place between the magnetized solar wind plasma outflow from the Sun and celestial bodies in the solar system. Magnetized planets form magnetospheres in the solar wind, with the planetary field creating an obstacle in the flow. All these magnetospheres have the same structure, consisting of several magnetic field sources, but there are differences between magnetospheres. In our work we have refined models of the magnetospheres of four solar system planets on the basis of the Paraboloid magnetospheric model. The analysis shows that the task of building a generalized model of the planet's magnetosphere is both relevant and feasible. At our disposal, there are more than 60 years of direct studies of the Earth's magnetosphere and the AMC flights to the planets of the solar system made during this time with the withdrawal of spacecraft into the orbits of the satellites of Mercury, Jupiter and Saturn. We confine ourselves to those planets that have been studied by a spacecraft and have a noticeable intrinsic magnetic field that forms a cavity in the plasma flow of the solar wind — the planet's magnetosphere.

We limited ourselves to only four planets of the solar system, since the rest of the planets with a strong magnetic field have not yet been directly studied by AMCs operating on satellite orbits. At the same time, on the one hand, the mechanisms of plasma interaction with the planetary magnetic field are quite versatile and allow us to construct models of the planetary magnetospheres, repelling the relatively extensively studied Earth's magnetosphere. On the other hand, the range of changes in the size of the magnetospheres is from the giant magnetosphere of Jupiter (about 8 million kilometres to the subsolar point of the magnetopause, or 0.05 AU, while the tail of the Jupiter magnetosphere is 100 times larger - about 5 AU) to the miniature Mercury magnetosphere (3.4 thousand km to the nose point on the magnetopause and the tail of the magnetosphere is about 10 times longer than the distance to the subsolar magnetopause). Mercury and Saturn magnetosphere model parameters are included into VESPA environment through EPN-TAP.

## **1. Upgrade the paraboloid magnetospheric models of the solar system planets**

### **1.1 Introduction and goals**

A wide variety of interactions takes place between the magnetized solar wind plasma outflow from the Sun and celestial bodies in the solar system. Magnetized planets form magnetospheres in the solar wind, with the planetary field creating an obstacle in the flow. All these magnetospheres have the same structure, consisting of several magnetic field sources, but there are differences between magnetospheres. In our work we have refined models of the magnetospheres of four solar system planets on the basis of the Paraboloid magnetosphere model. Web-portal <http://www.magnetosphere.ru> allows to calculate magnetospheric magnetic field of four planets in the Solar system which have magnetospheres - Mercury, Earth, Saturn and Jupiter for different conditions in space environment. The main aim of this work is to include magnetosphere models parameters into VESPA environment through EPN-TAP.

### **1.2 Implementation**

#### **1.2.1 Input data structure for Hermean magnetosphere**

Data files contain parameters of Hermean magnetosphere for compressed, quiet and expanded magnetosphere

	BD	BT	RSS	R2	DZ	IMF Bx	IMF By	IMF Bz
Compressed	192nT	165nT	1.21Rm	1.25Rm	0.095Rm	27nT	-2nT	20nT
Quiet	192nT	173nT	1.33Rm	1.35Rm	0.32Rm	-33nT	-12nT	21nT
Expanded	192nT	95nT	1.56Rm	1.25Rm	-0.65Rm	24nT	-3nT	22nT

Model input parameters:

- BD - Dipole field strength on the equator of the Mercury;
- BT - Magnetic flux at the inner edge of magnetospheric tail current sheet;
- RSS - Subsolar magnetopause distance in the Mercury radii (2439km);
- R2 – The distance to the inner edge of the tail current sheet;
- DZ - Northern displacement of the dipole relative to the center of the Mercury;
- IMF\_B - Components of the Interplanetary Magnetic Field penetrated into the Mercury's magnetosphere (in the HSM coordinate system).

### 1.2.2 Input data structure for Saturn magnetosphere

Data files contain parameters of Saturn's magnetosphere for compressed, quiet and expanded magnetosphere

	BDC	BT	RSS	R2	RD1	RD2	IMF Bx	IMF By	IMF Bz
Compressed	3.62nT	8.7nT	17.5Rs	14Rs	12.5Rs	6.5Rs	0.5nT	-2nT	-1.4nT
Quiet	3nT	7nT	22Rs	18Rs	15Rs	6.5Rs	-0.3nT	0.7nT	0.7nT
Expanded	2.2nT	5.3nT	28Rs	22.45Rs	24.5Rs	6.5Rs	0nT	-0.4nT	-0.4nT

Model input parameters:

- BDC - Magnetic field at the magnetodisc (MD) outer edge
- BT - Minus Z-component of the magnetic field at the tail current sheet inner edge
- RD2 - Distance to the inner edge of the MD
- RD1 - Distance to the outer edge of the MD
- R2 - Distance to the inner edge of the tail current sheet
- Rss - Magnetopause stand-off distance
- IMF\_B - Components of the Interplanetary Magnetic Field penetrated into the magnetosphere in the KSM coordinate system

### 1.2.3 Coronas-F data

Data files contain measurements of energetic particle fluxes by MKL instrument onboard Russian Coronas-F satellite from 2001-08-15 till 2003-12-31. Data structure has been described in D6.18

### 1.2.4 Data location

Coronas-F data measurements are collected in CDF format.

- Direct URL: <http://vespa.sinp.msu.ru:8080/data/coronas>
- DaCHS server URL: <http://vespa.sinp.msu.ru/>
- EPN-TAP URL [http://vespa.sinp.msu.ru/system /tap/run/tap](http://vespa.sinp.msu.ru/system/tap/run/tap) with table name

- “coronasf.epn\_core”
- ADQL Query URL: <http://vespa.sinp.msu.ru/system/adql/query/form>

### **1.2.5 Access to data**

Data can be accessed by two different ways. The first is direct http access to daily CDF files and the second one is using EPN-TAP protocol with URL [http://vespa.sinp.msu.ru/\\_system/tap/run/tap](http://vespa.sinp.msu.ru/_system/tap/run/tap) by one of the available compatible software (TOPCAT for example).

Paraboloid models parameters for Mercury and Saturn are stored in DaCHS server and available through EPN\_TAP service and ADQL Query URL mentioned above with table names “parameters\_mercury.epn\_core” and “parameters\_saturn.epn\_core”, respectively.

## **2. Upgrade the paraboloid magnetospheric models of the Solar system planets.**

The short list of main achievements for 2017-2019 years is:

### **2.1 The combined model of Mercury’s magnetosphere**

The combined model (comprised of a numerical hybrid simulation and the empirical paraboloid model) of Mercury’s magnetosphere has been developed. It gives us the possibility to refine the global parameters of magnetosphere using MESSENGER’s magnetometer data from each of over 4100 orbits of the spacecraft around Mercury (see [Parunakyan et al., 2017]).

We have performed calculations of the initial magnetospheric magnetic field of Mercury and the boundary conditions for subsequent hybrid modeling and defined the initial parameters of the global magnetospheric current systems in a way that allows us to minimize paraboloid magnetic field deviation along the trajectory of MESSENGER from the experimental data. We have modelled the magnetosheath magnetic field and calculated the portion of the interplanetary magnetic field penetrating the magnetosphere (see [Alexeev et al., 2017]).

Solar wind variations, changes of the magnetospheric current systems – both of these factors lead to the fact that the magnetic field in the magnetosphere varies with time. One of the ways to describe these changes is to change the parameters of the current systems from one revolution of MESSENGER to another, assuming that the state of the magnetosphere is stationary for about an hour, and the parameters of the magnetosphere can change from one revolution to another. With the data of the magnetometer along the trajectory of the spacecraft, it is possible to find the parameters of magnetospheric current systems using the maximum likelihood method, looking for a minimum of the sum of squared differences of predicted and measured field components.

The program for searching for the minimum of this sum used the magnetometer data obtained on the MESSENGER trajectory around Mercury. The program for the model field calculation was based on a paraboloid model with free parameters, which makes it possible to calculate the magnetic field in the planet’s magnetosphere and compare it with the experimental data obtained. In addition to this program, it was necessary to write and debug a program shell capable of interacting with the FUMILIM package. The author of this package participated in the processing of the MESSENGER data obtained when flying around Mercury during gravitational maneuvers at the stage of spacecraft transfer to the orbit of the Mercury satellite. This package was not designed to work with vector functions, the discrepancies for the individual components of the magnetic field vector were considered as independent variables. One of the tasks that had to be

solved during the execution of the project required an assessment of the computing resources necessary to solve the optimization problem, including the estimation of processor time for calculating one orbit of MESSENGER. This assessment will answer the question about the possibility of developing a program that will work in real time, calculating the parameters of the model during the flight of the spacecraft.

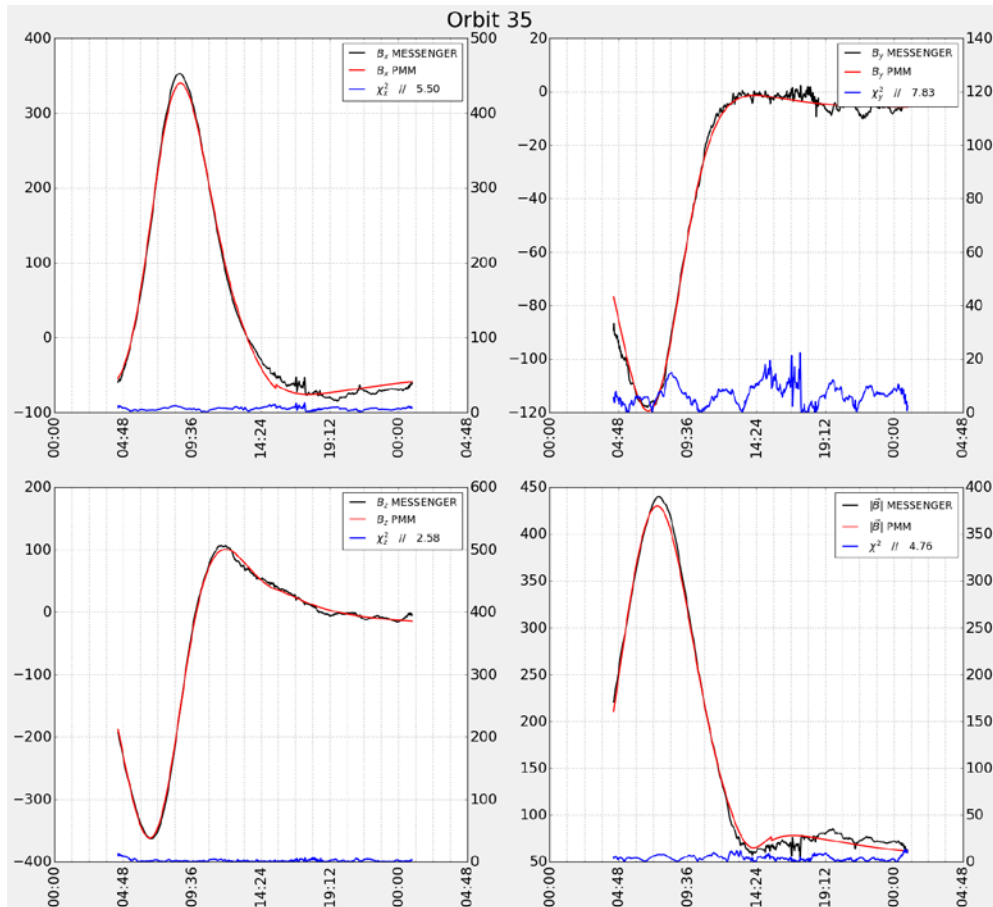


Figure 1. The experimental data and the results of data processing using paraboloid model for one orbit for the three components of the magnetic field. At such a scale, due to the density of experimental points, it is difficult to distinguish the model and experimental curves.

The main task was to find the parameters that determine the planetary magnetic field of Mercury ( $N_{\text{global}} = 6$ ). In the first approximation, neglecting the secular variations, we considered these parameters as constant during the transition from one orbit to another. In addition, each orbit is characterized by local parameters ( $N_{\text{local}} = 7$ ), which describe the state of the magnetospheric current systems formed during the interaction of the solar wind plasma with the planetary field. As a result of fitting the magnetic field vector data parameters of the Paraboloid model for Mercury for different MESSENGER orbits have been determined. Parameters, R1 (distance to the subsolar point) and R2 (distance to the tail current sheet) do not differ much for different orbits, which indicates the likelihood of the results obtained. This allows us to hope that the proposed method will make it possible to isolate the temporal dynamics of the magnetosphere and limit the number of actual parameters describing its dynamics.

## 2.2 Jovian magnetosphere modeling

One of the main features of Jupiter's magnetosphere is its equatorial magnetodisc, which significantly increases the field strength and size of the magnetosphere. Analysis of Juno measurements of the magnetic field during the first 10 orbits covering the dawn to pre-dawn sector

of the magnetosphere ( $\sim 03:30\text{--}06:00$  local time) has allowed us to determine optimal parameters of the magnetodisc using the paraboloid magnetospheric magnetic field model, which employs analytic expressions for the magnetospheric current systems. Specifically, within the model we determine the size of the Jovian magnetodisc and the magnetic field strength at its outer edge.

Juno measurements of the magnetic field during the Perijove 1 pass have allowed us to determine optimal parameters of the magnetodisc using the paraboloid magnetospheric magnetic field model which employs analytic expressions for the magnetospheric current systems. Specifically, within the model we determine the size of the Jovian magnetodisc and the magnetic field strength at its outer edge [Pensionerov et al., 2019]. We have also studied alternative magnetodisc descriptions, including the  $1/r$  azimuthal current density dependence on the radial distance to the planet and  $1/r^2$  dependence. We have modeled the magnetic field observations during Juno's first 10 orbits for which both inbound and outbound passes are presently available, corresponding to perijoves (PJs) 0 to 9, using the semi-empirical global paraboloid Jovian magnetospheric magnetic field model. We focus on the middle magnetosphere, observed on these orbits in the dawn to pre-dawn sector of the magnetosphere ( $\sim 03:30\text{--}06:00$  local time, LT), for which the magnetodisc provides the main contribution to the magnetospheric magnetic field. In the model, in which the field contributions are calculated using parameterized analytic equations, the magnetodisc is described by a simple thin plane disc lying in the planetary magnetic equatorial plane. We thus search the paraboloid model magnetodisc input parameters to determine the best fit to the Juno measurements. We note that the magnetodisc may be regarded as the most important source of magnetic field in Jupiter's magnetosphere, with a magnetic moment in the model derived by Alexeev and Belenkaya (2005), DOI:10.5194/angeo-23-809-2005, using Ulysses inbound data, for example, which is 2.6 times the planetary dipole moment. Consequently, the magnetodisc plays a major role in determining the size of the magnetosphere in its interaction with the solar wind and is thus an appropriate focus of a study using Juno magnetic field data.

The paraboloid magnetospheric magnetic field model for Jupiter contains the internal planetary field,  $B_i$ , calculated from the full order-4 VIP4 model of Connerney et al. (1998); the magnetodisc field,  $B_{MD}$ ; the field of the magnetopause shielding currents,  $B_{Si}$  and  $B_{SMD}$ , which screen the planetary and magnetodisc fields, respectively; the field of the magnetotail current system,  $B_{TS}$ ; and the penetrating part of the interplanetary magnetic field (IMF),  $k \cdot B_{IMF}$ , where  $k$  is the IMF penetration coefficient. The magnetopause is described by a paraboloid of revolution in Jovian solar magnetospheric (JSM) coordinates with focus at Jupiter's center.

Also, we developed a new empirical model of Jupiter's equatorial current sheet or magnetodisc, constructed by combining appropriate elements from several previous models. The new model employs a disk-like current of constant north-south thickness in which the current density is piecewise dependent on the distance  $r$  from Jupiter's dipole axis, proportional to  $r^{-1}$  at distances between  $\sim 7$  and  $\sim 30 R_J$  and again at distances between  $\sim 50$  and  $\sim 95 R_J$ , and to be continuous in value but proportional to  $r^{-2}$  at distances between these regions. For this reason, the model was named the Piecewise Current Disk model. The model also takes into account magnetodisc bending with distance and azimuthal curvature due to finite radial propagation speed and solar wind effects. It is taken to be applicable in the radial distance range between  $\sim 5$  and  $\sim 60 R_J$ . Optimized parameters have been determined for Juno magnetic field data obtained on Perijove-01, with the model showing overall the lowest root-mean-square deviation from the data compared with similarly optimized earlier models.

Figure 2. Cross section of the model current sheet in the  $\phi = \pi/4$  meridian plane, showing color coded azimuthal current density for the PCD model, calculated from curl B. The solid lines show the field lines of the PCD model combined with the JRM09 internal field of Connerney et al. (2018). The dashed line shows the current sheet center. PCD = Piecewise Current Disk.

Figure 3. Comparison of the poloidal fields calculated from the PCD model (orange line) and the observed residual field on Juno Perijove-01 from which the JRM09 internal field has been subtracted (black line). (a, b) The cylindrical  $\rho$  and  $z$  field components, respectively. The fields are plotted versus radial distance  $r$  from the planet's center with data from the inbound and outbound trajectories being shown to the left and right of the origin, respectively. The part of the trajectory where the field of the current disk becomes indistinguishable on the background of the internal field is marked by the gray band as "not distinguishable". PCD = Piecewise Current Disk.

Figure 4. RMS error of the models in the inner, middle, and outer regions of the Juno Perijove-01 trajectory. PCD = Piecewise Current Disk; RMS = root-mean-square.

### **2.3 Saturn magnetosphere modeling**

We have continued our work on the determination of the main features of Saturn's magnetosphere using Cassini magnetic field data. We have compared 2012/2013 Saturn northern spring interval of highly inclined orbits with similar data from late southern summer in 2008, thus providing unique information on the seasonality of the currents that couple momentum between Saturn's ionosphere and magnetosphere.

Inferred meridional ionospheric currents in both cases consist of a steady component related to plasma subcorotation, together with the rotating current systems of the northern and southern planetary period oscillations. This helped us to develop a correct model of the field-aligned currents in the magnetosphere (see [Bradley et al., 2018]).

We have also considered two magnetospheric magnetic field models for the case of Saturn: an open model in which the IMF penetrates the magnetosphere, and a partially closed model in which field lines from the ionosphere go to the distant tail and interact with the solar wind at its end. The reconnection efficiency of the solar-wind-magnetized planet interaction depends on the conditions in the magnetized plasma flow passing the planet. When the reconnection efficiency is very low, the interplanetary magnetic field (IMF) does not penetrate the magnetosphere, a condition that has been widely discussed in the recent literature for the case of Saturn. We have studied this issue for Saturn using Cassini magnetometer data, images of Saturn's ultraviolet aurora obtained by the HST, and the paraboloid model of Saturn's magnetospheric magnetic field. Two models were considered: first, an open model in which the IMF penetrates the magnetosphere, and second, a partially closed model in which field lines from the ionosphere go to the distant tail and interact with the solar wind at its end. We have concluded that the open model is preferable, which is more obvious for southward IMF. For northward IMF, the model calculations do not allow us to reach definite conclusions. However, analysis of the observations available in the literature provides evidence in favor of the open model in this case too. The difference in magnetospheric structure for these two IMF orientations is due to the fact that the reconnection topology and location depend on the relative orientation of the IMF vector and the planetary dipole magnetic moment. When these vectors are parallel, two-dimensional reconnection occurs at the low-latitude neutral line. When they are antiparallel, three-dimensional reconnection takes place in the cusp regions. Different magnetospheric topologies determine different mapping of the open-closed boundary in the ionosphere, which can be considered as a proxy for the poleward edge of the auroral oval.



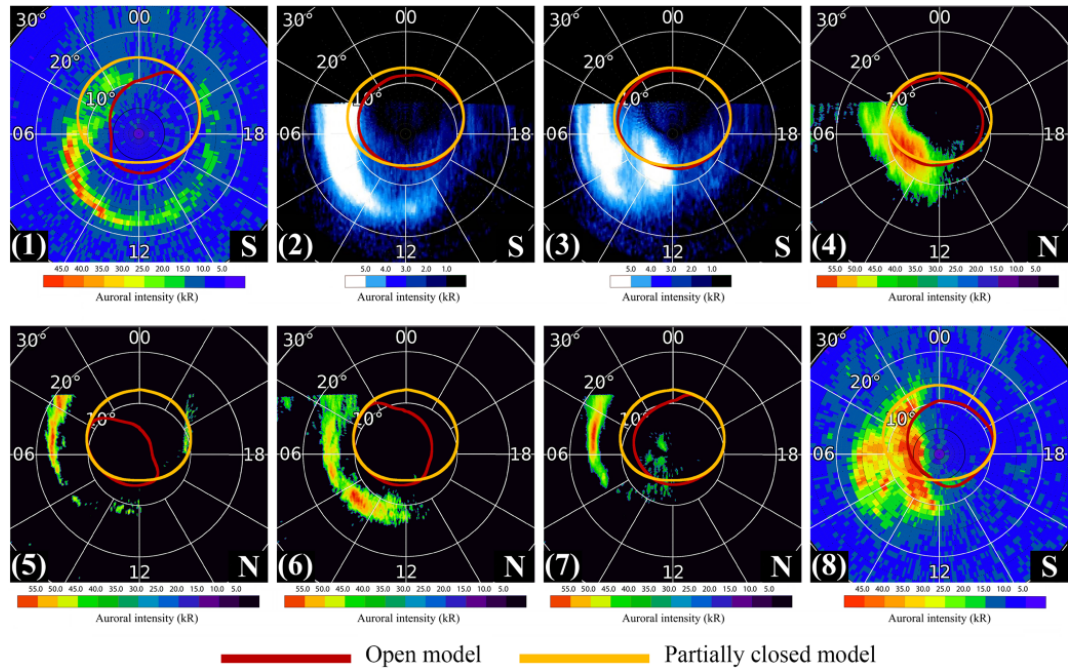


Figure 5. Saturn UV auroral images obtained by the HST for southward IMF, with noon on the bottom and dusk on the right. The closed red curve in all figures in this paper shows the open flux boundary for the open magnetosphere model with  $k = 0.2$  using a multipole Saturn magnetic field (Burton et al., 2010) and a spheroidal ionosphere. The closed orange curve in all figures in this paper shows the open flux boundary for the partially closed model in which the IMF does not penetrate the magnetopause.

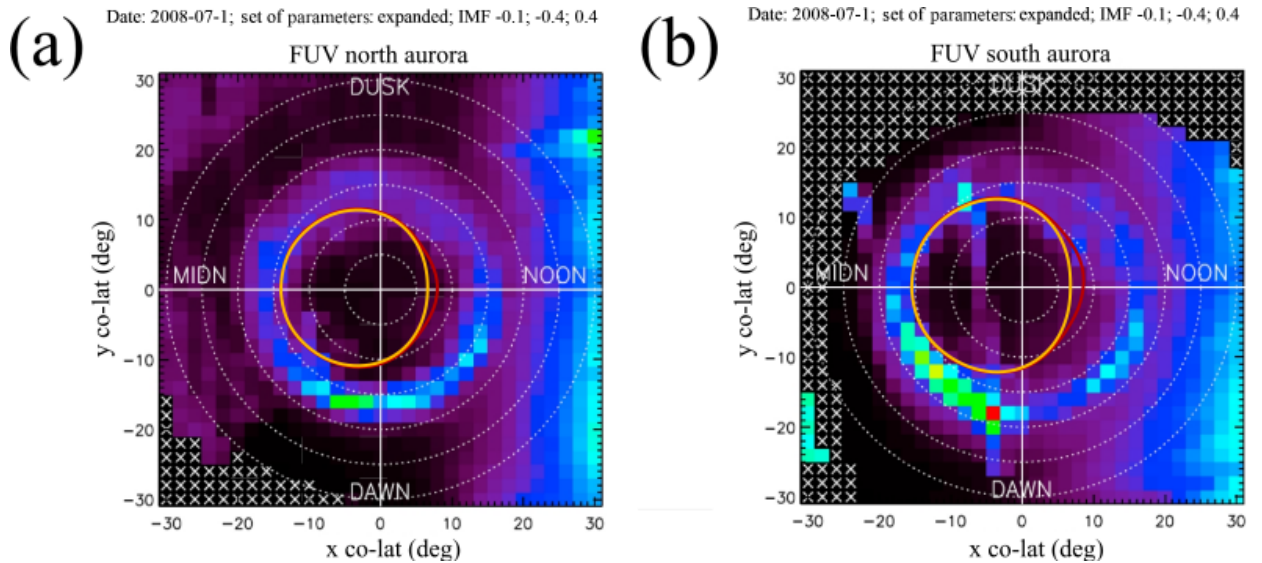


Figure 2. Comparison of the statistical UV auroral oval obtained by Carbary (2012) from Cassini UVIS data from 2007–2009 with model calculations of the open-closed field line boundary for (a) the northern and (b) the southern hemispheres. The model time was selected to be 1 July 2008 (the middle of the interval of Cassini observations), and the set of the model parameters corresponds to the expanded state of the magnetosphere, i.e., low solar wind dynamic pressure (see text). The northward-directed IMF vector assumed has components  $(-0.1, -0.4, 0.4)$  nT. The red line marks the open flux boundary for the open model, while the orange line is for the partially closed model.

The paraboloid model of Saturn's magnetosphere describes the magnetic field as being due to the sum of contributions from the internal field of the planet, the ring current, and the tail current, all contained by surface currents inside a magnetopause boundary which is taken to be a paraboloid of revolution about the planet-Sun line. The parameters of the model have previously been determined by comparison with data from a few passes through Saturn's magnetosphere in compressed and expanded states, depending on the prevailing dynamic pressure of the solar wind.

We significantly expanded such comparisons through examination of Cassini magnetic field data from 18 near-equatorial passes that span wide ranges of local time, focusing on modelling the co-latitudinal field component that defines the magnetic flux passing through the equatorial plane. For 12 of these passes, spanning pre-dawn, via noon, to post-midnight, the spacecraft crossed the magnetopause during the pass, thus allowing an estimate of the concurrent subsolar radial distance of the magnetopause  $R_1$  to be made, considered to be the primary parameter defining the scale size of the system. The best-fit model parameters from these passes are then employed to determine how the parameters vary with  $R_1$ , using least-squares linear fits, thus providing predictive model parameters for any value of  $R_1$  within the range. We showed that the fits obtained using the linear approximation parameters are of the same order as those for the individually selected parameters. We also show that the magnetic flux mapping to the tail lobes in these models is generally in good accord with observations of the location of the open-closed field line boundary in Saturn's ionosphere, and the related position of the auroral oval. We then investigated the field data on six passes through the nightside magnetosphere, for which the spacecraft did not cross the magnetopause, such that in this case we compared the observations with three linear approximation models representative of compressed, intermediate, and expanded states. Reasonable agreement was found in these cases for models representing intermediate or expanded states.

All this results can be found in [Belenkaya et al., 2016; 2017].

Model parameter	Compressed case $p_{sw} \sim 0.08$ nPa	Intermediate case $p_{sw} \sim 0.03$ nPa	Expanded case $p_{sw} \sim 0.01$ nPa
$R_1$ ( $R_S$ )	17.5	22	28
$R_{rc1}$ ( $R_S$ )	12.5	15	24.5
$R_{rc2}$ ( $R_S$ )	6.5	6.5	6.5
$B_{rc1}$ (nT)	3.62	3	2.2
$I_\varphi$ (MA)	4.0	5.6	14.3
$R_2$ ( $R_S$ )	14	18	22.45
$B_t$ (nT)	8.7	7	5.3

Table 1. Paraboloid model parameter sets for compressed, intermediate, and expanded Saturn magnetospheric states, following Alexeev et al. (2006) and Belenkaya et al. (2006b, 2008), together with the total current flowing in the ring current given by Eq. (2).

## Bibliography

- Alexeev I., Parunakian, D., Dyadechkin, S., Belenkaya, E., Khodachenko, M, Kallio, E, Alho M, Calculation of the Initial Magnetic Field for Mercury's Magnetosphere Hybrid Model . Cosmic Res (2018) 56: 108. <https://doi.org/10.1134/S0010952518020028>
- Belenkaya, E. S., Kalegaev, V. V., Cowley, S. W. H., Provan, G., Blokhina, M. S., Barinov, O. G., Kirillov, A. A., and Grigoryan, M. S.: Optimization of Saturn paraboloid magnetospheric field model parameters using Cassini equatorial magnetic field data, Ann. Geophys., 34, 641-656, <https://doi.org/10.5194/angeo-34-641-2016>, 2016
- Belenkaya, E. S., Cowley, S. W. H., Alexeev, I. I., Kalegaev, V. V., Pensionerov, I. A., Blokhina, M. S., and Parunakian, D. A.: Open and partially closed models of the solar wind interaction with outer planet magnetospheres: the case of Saturn, Ann. Geophys., 35, 1293-1308, <https://doi.org/10.5194/angeo-35-1293-2017>, 2017
- Bradley, T. J., Cowley, S. W. H., Provan, G., Hunt, G. J., Bunce, E. J., Wharton, S. J., Alexeev, I. I., Belenkaya, E.S., Kalegaev, V.V., Dougherty, M.K. (2018), Field-aligned currents in

Saturn's nightside magnetosphere: Subcorotation and planetary period oscillation components during northern spring. *Journal of Geophysical Research: Space Physics*, 123, 3602–3636, <https://doi.org/10.1029/2017JA024885>

Parunakian, D., S. Dyadechkin, I. Alexeev, E. Belenkaya, M. Khodachenko, E. Kallio, and M. Alho (2017), Simulation of Mercury's magnetosheath with a combined hybrid-paraboloid model, *J. Geophys. Res. Space Physics*, 122, 8310–8326, doi: 10.1002/2017JA024105

Pensionerov, I. A., Belenkaya, E. S., Cowley, S. W. H., Alexeev, I. I., Kalegaev, V. V., and Parunakian, D. A.: Magnetodisc modelling in Jupiter's magnetosphere using Juno magnetic field data and the paraboloid magnetic field model, *Ann. Geophys.*, 37, 101-109, <https://doi.org/10.5194/angeo-37-101-2019>, 2019